Supplementary Materials for "Turbidity in Apalachicola Bay, Florida from Landsat5 TM and field data: Seasonal patterns and response to extreme events" by Ishan D. Joshi, Eurico J. D'Sa, Christopher L. Osburn, Thomas S. Bianchi

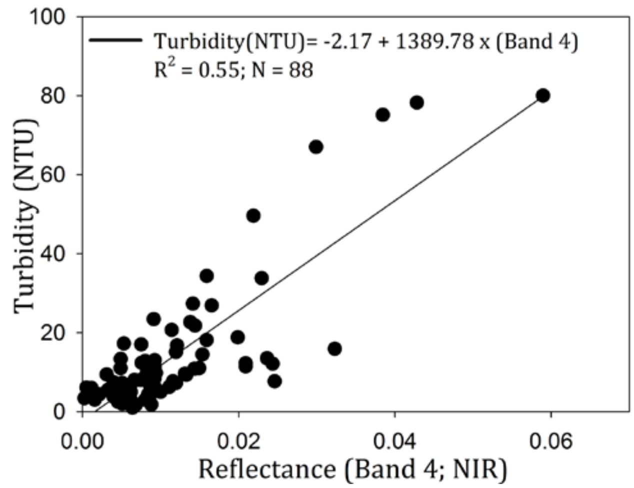

Figure S1: Landsat5 TM turbidity algorithm with NIR band (Band 4).

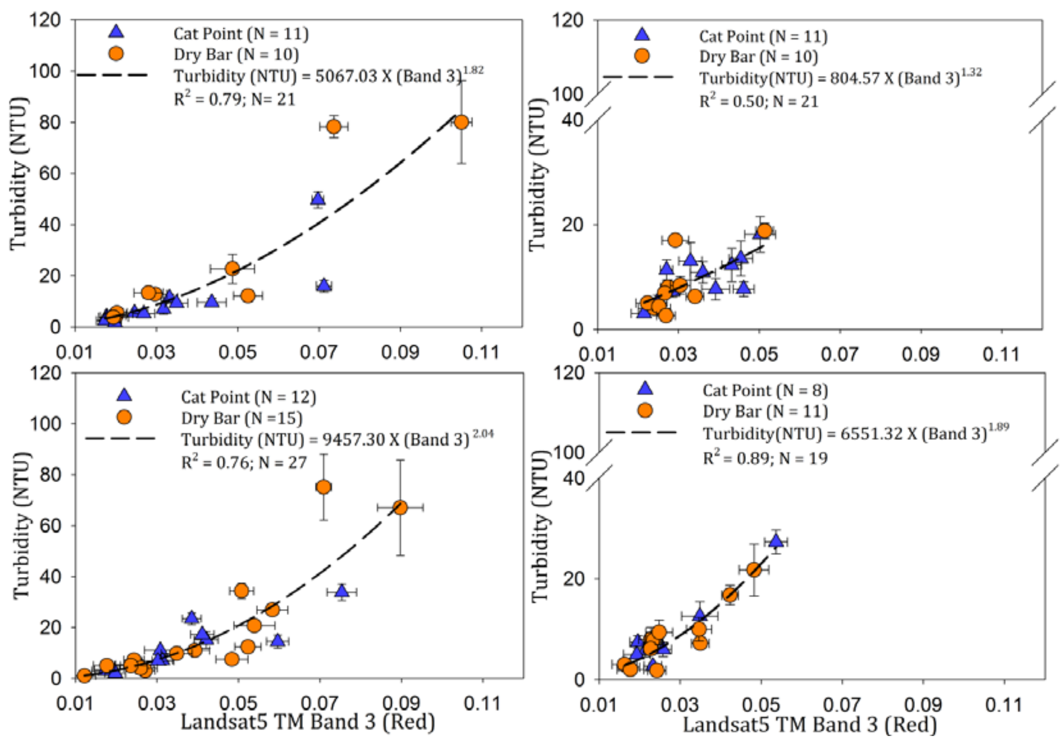

Figure S2: Turbidity-Landsat5 TM relationships for different seasons. Blue and orange symbols represent measurements at Cat Point and Dry Bar stations.

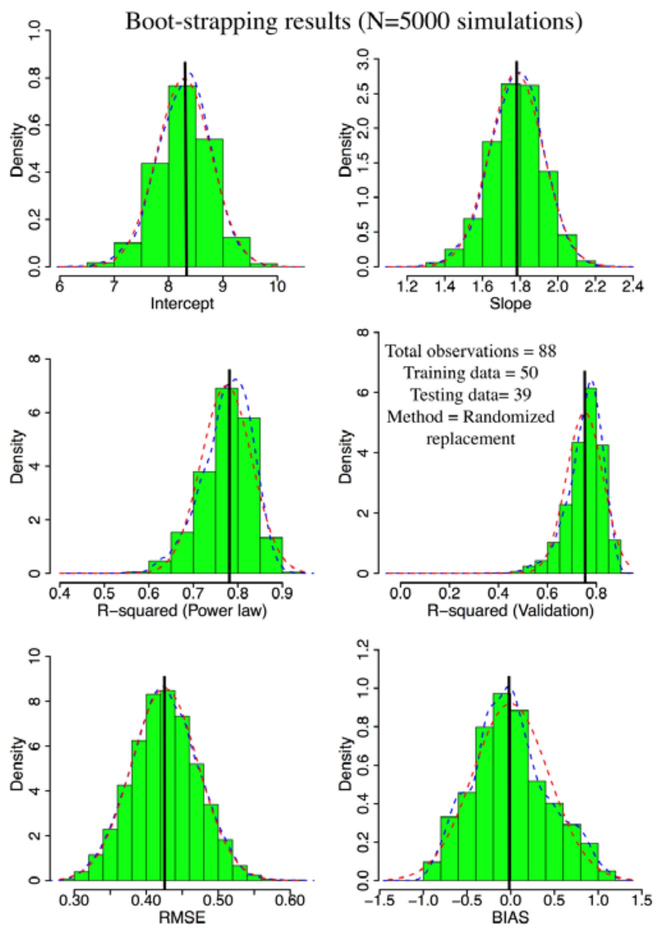

Figure S3: Bootstrap simulation (N=5000) results, a) intercept or log (constant) (Mean ± SD = 8.32 ± 0.50, range = 6.2 - 10.16), b) slope or power law exponent (Mean ± SD = 1.76 ± 0.14, range = 1.16 – 2.35), c) R^2 for turbidity-Landsat5 TM algorithm, d) R^2 for algorithm validation, e) RMSE for algorithm validation, and f) bias for algorithm validation. Blue and red curves represent probability and normal distributions, respectively.

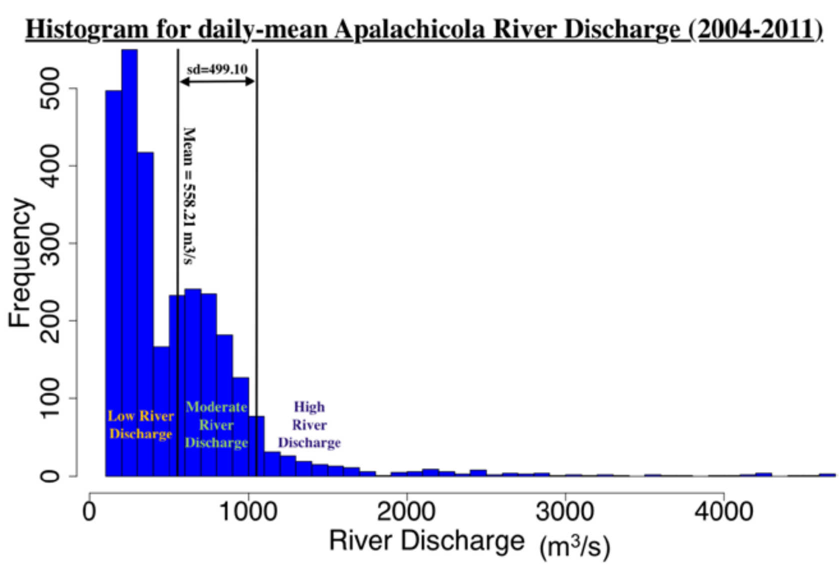

Figure S4: Histogram of mean-daily Apalachicola River discharge from 2004 to 2011.

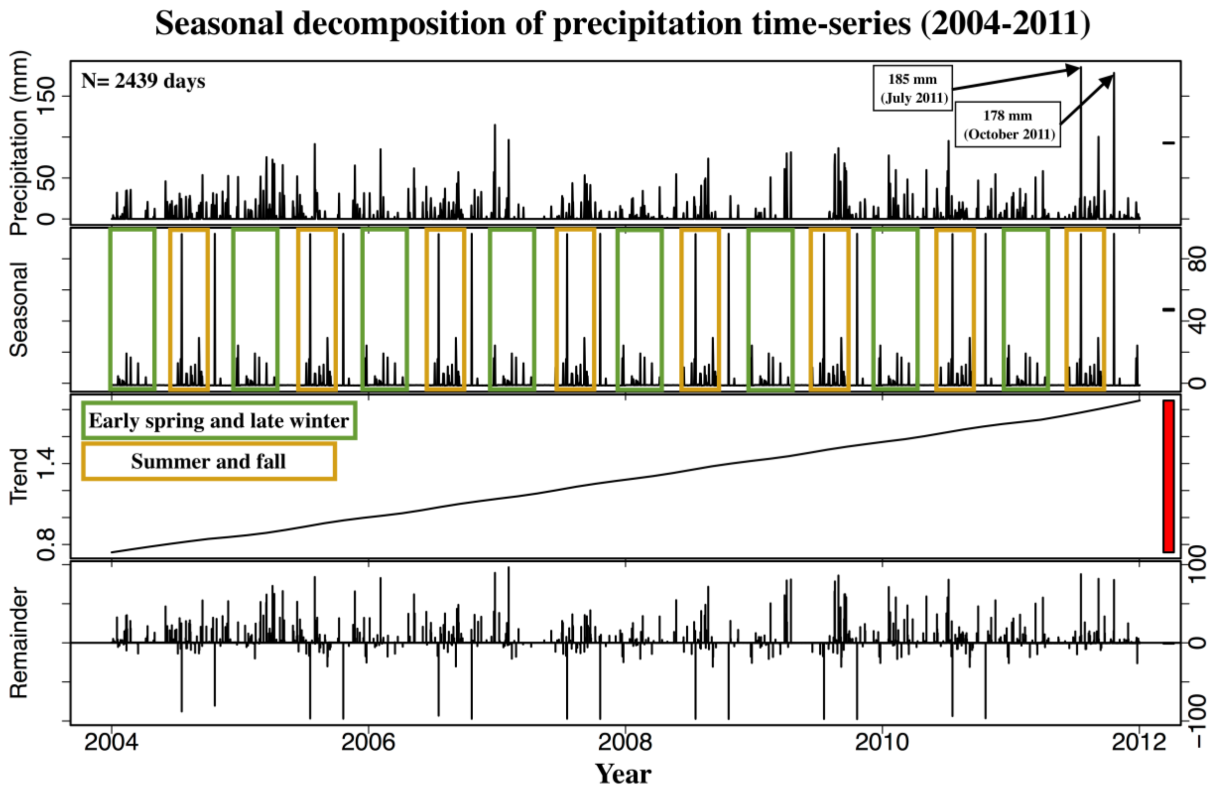

Figure S5: Decomposition of precipitation time-series (2004 – 2011) into, a) daily (N = 2439 days), b) seasonal, c) yearly trend, d) random or remainder component (=daily time-series - (seasonal component + yearly trend)). Units, in millimeters, can be compared to the original time-series based on the length of bar located to the right side of each panel, *e.g.*, the longer bar indicates low contributions to the original time-series and vice-versa. The remainder component contributed the most to the precipitation time-series. The seasonal component is another important contributor to the precipitation time-series that showed relatively strong precipitation in late winter and early spring, possibly due to the convection activities corresponding to the progression of frontal systems towards the warm Gulf waters (green boxes). Furthermore, it showed that the bay experienced frequent events of rainfall in summer and fall that could be associated to surface-water heating, thunderstorms, and tropical storms (yellow boxes). The thick red bar and small precipitation values indicated that there was no distinct yearly-trend in precipitation from 2004 to 2011. The hurricanes during years 2004 and 2005, the costliest and active Atlantic hurricane seasons in history, can be linked with times that the bay received significant amount of perceptible water inputs, *e.g.*, HCs Frances, Ivan, and Jeanne in September, 2004, and TS Arlene, HCs Dennis, Cindy, and Katrina in July – August, 2005 (also see Figure 6f). [**Note:** The remainder time-series also showed two distinct negative peaks each year similar to the two positive peaks in the seasonal component. Apalachicola Bay experienced two strong precipitation events in 2011, and these anomalies could have introduced a noise in the seasonal component that propagated further to the remainder.]

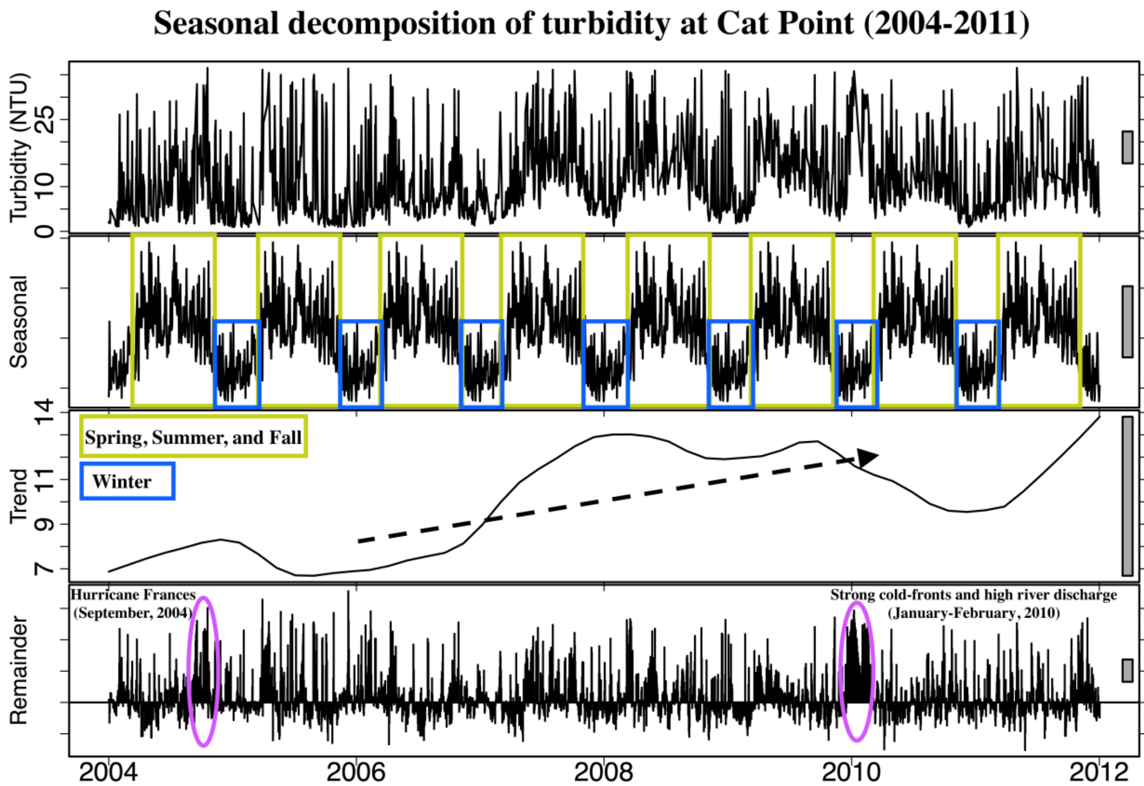

Figure S6: Time-series of turbidity was decomposed into seasonal, trend, and random components for recognizing the underlying pattern during the 8-years of study period at Cat Point station. While the remainder component was the major contributor to the turbidity time-series, a seasonal trend at Cat Point showed relatively higher turbidity in spring, summer and fall seasons (green boxes), in contrast to low turbidity in winter (blue box). The magnitude of the yearly trend was not comparable to seasonal and remainder components, however, it did show an increasing trend of turbidity at Cat Point. Similar yearly trends were observed at Dry Bar, with relatively turbid waters in the years 2004, 2008, and 2010, and relatively clear waters in the years 2006 and 2011 – when the influence of extreme weather events was removed from the analysis.

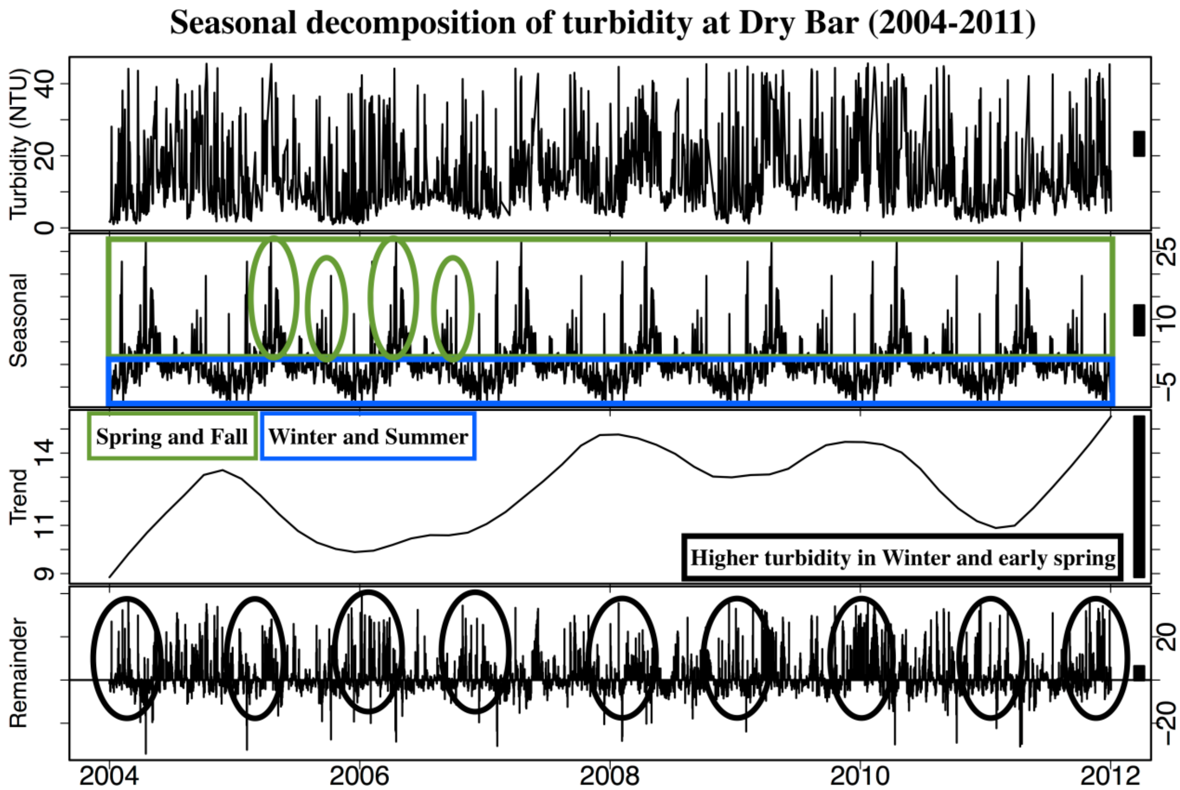

Figure S7: The turbidity time-series at Dry Bar was decomposed after removing outliers (high turbidity due to cold fronts, thunderstorms, Apalachicola River floods, hurricanes etc.). The remainder component was the major contributor to the turbidity variations followed by the seasonal and trend components. Erratic behavior in daily turbidity time-series could be attributed to the daily tidal-cycle and wind-induced sediment re-suspension. A seasonal component generally showed a harmonic pattern with two peaks (large one in spring and small in fall) and two troughs (large one in the winter and a small summer). Although seasonal component indicated low turbidity in winter, strong turbidity peaks in the remainder can be attributed to the wind-driven water mixing during the frontal passages, other than due to the river discharge in late winter and early spring in Apalachicola Bay (black ellipses, A3). Mean-yearly water turbidity was of less important however, it showed that the Dry Bar station experienced moderately turbid waters in the years 2004, 2008, and 2010, and relatively clear waters in the years 2006 and 2011 - when the influence of extreme weather events was removed from the analysis.

Table S1: Bootstrapping statistics for the turbidity algorithm and its validation.

Bootstrapping statistics (N = 5000 simulations, Total data = 88) Data selection = *Randomized replacement*					
	Mean	Standard deviation	Median	Minimum	Maximum
Turbidity algorithm **:- ln (Turbidity) = Intercept + Slope × ln (Band 3)** (train data = 50)					
Intercept	8.22	0.50	8.24	5.81	10.16
Slope	1.76	0.14	1.77	1.09	2.35
R^2	0.77	0.06	0.78	0.50	0.91
Algorithm Validation (test data = 38)					
R^2	0.70	0.15	0.72	-0.96	0.97
RMSE	7.78	2.59	7.78	2.24	17.10
Bias (%)	-8.70	11.48	-9.44	-43.48	49.50

Table S2: Sample size, mean, standard deviation, and range of mean-daily river discharge, precipitation, salinity, tidal height, wind speed, water depth, and turbidity from 2004 to 2011 in Apalachicola Bay. MLLW = Tidal datum as Mean-Low Low-Water.

Descriptive statistics					
Variable	Number of samples	Mean	Standard deviation	Maximum	Minimum
River Discharge (m^3s^{-1})	2922	558.21	499.10	4697.81	124.52
Precipitation (mm)	2439	2.97	11.15	185.42	0
Salinity	2922 (Cat Point)	21.69	7.78	37.57	0.10
	2922 (Dry Bar)	21.99	7.45	38.58	0.11
Tidal height (m) above MLLW (MLLW=1.307m)	2922	0.28	0.06	0.38	0.17
Wind speed (ms^{-1})	2877	2.67	1.06	12.83	0.49
Depth (m)	2922 (Cat Point)	2.03	0.40	3.26	1.46
	2838 (Dry Bar)	1.71	0.37	3.00	1.05
Turbidity (NTU)	2758 (Cat Point)	16.94	29.48	511.98	1
	2765 (Dry Bar)	21.09	32.54	704.36	1

Table S3: Turbidity matchups at Cat Point and Dry Bar stations used to evaluate applicability of the Landsat5 TM-based turbidity algorithm to Landsat8 OLI images (17 images). Highlighted images were used to generate turbidity maps in section 4.

Date	Turbidity at Cat Point (NTU)	Turbidity at Dry Bar (NTU)	Horizontal Visibility (km)
October 06, 2014	5.2	4.7	66.4
October 22, 2014	9.4	5.2	57.5
November 07, 2014	6.0	4.8	91.7
November 14, 2014	4.2	9.6	55.6
November 30, 2014	1.7	2.6	43.2
December 09, 2014	7.2	8.9	92.5
January 26, 2015	25.9	-	39.4
February 11, 2015	3	4.7	146.1
February 18, 2015	9.0	6.7	51.2
May 02, 2015	8.6	16.1	57.2
November 26, 2015	13.4	30.9	43.9
December 12, 2015	-	4.3	56.3
December 19, 2015	12.6	-	62.9
March 08, 2016	10.2	35.6	37.4
May 04, 2016	8.8	25.6	27.3
July 07, 2016	9.6	6.2	43.1
July 23, 2016	6.6	10.7	34.9